BIOGENIC SYNTHESIS OF FERROUS(III) OXIDE AND Fe$_3$O$_4$/SiO$_2$ USING *CHLORELLA* sp. AND ITS ADSORPTION PROPERTIES OF WATER CONTAMINATED WITH COPPER(II) IONS

Shireen Ibrahim Hamadamin[1], Sewgil Saaduldeen Anwer[1,2*], Parween Mohsin Abdulkareem[3] and Kwestan Hassan Sdiq[4]

[1]Hawler medical University-College of Health Sciences/Clinical Biochemistry Department, Kurdistan Region, Iraq
[2]Tishk International University, Nursing Faculty, Nursing Department, Kurdistan Region, Iraq
[3]Department of Biology, Faculty of Science and Health, Koya University, Koya KOY45, Kurdistan Region, Iraq
[4]Hawler Medical University, College of Health Sciences/Medical Microbiology Department, Kurdistan Region, Iraq

ABSTRACT. Magnetic nanoparticles (MNPs) are gaining popularity because of their small size allowing for research into the fundamentals of magnetism. In wastewater treatment, adsorption methods commonly remove heavy metals, but copper (Cu^{+2}) ion removal using magnetic nanoparticles (NPs) has not been investigated. In this study two different modes were used to determine maximum adsorption capacity to remove copper(II). The nanoparticles containing the Fe$_3$O$_4$ with *Chlorella*, core-shell Fe$_3$O$_4$/SiO$_2$ with *Chlorella* sp. synthesized and characterized by Fourier transform infrared (FT-IR) analysis, the morphology observed by scanning electron microscope (SEM), crystalline structure, and grain size provided by energy dispersive X-ray (EDX) and X-ray diffraction (XRD). Copper(II) ion removal showed in both modes. The maximum copper(II) ion reduction percent was obtained by nanoparticles containing core-shell Fe$_3$O$_4$/*Chlorella* 80.3%, Fe$_3$O$_4$/SiO$_2$ with *Chlorella* sp. (86.9%) the result showed maximum removal using Fe$_3$O$_4$/SiO$_2$ with *Chlorella* sp. due to increase of surface area. The results indicate that the adsorption using magnetic nanoparticles with *Chlorella* sp. enhances the cell surface and provides easy access to the separation for both preparation and recapture.

KEY WORDS: Copper(II) ion, Magnetic nanoparticles, *Chlorella* sp., SiO$_2$ core-shell, Adsorption capacity percent

INTRODUCTION

Nanoscience is one of the most significant areas of current science research [1]. Magnetic nanoparticles (MNPs) have received increased interest for usage in biological applications such as nanobiotechnology and magnetic nanoparticles (MNPs) have peaked in environmental and medical applications such as magnetic resonance imaging (MRI), drug delivery systems, medical diagnostics water treatment [2-4]. In their bulk state, iron oxides are often inactive. By shrinking them to the nanoscale, they become a potential antibacterial agent. Surfaces coated with iron oxide nanoparticles inhibit Gram-positive and Gram-negative bacteria from adhering and colonizing [5].

The environmentally friendly creation of metallic nanoparticles using biological components has attracted attention. Zhang and his co-workers illustrated that green and useful synthetic methods had attracted great interest in which microbes and plants used to make nanoparticles that are biologically safe, cost-effective, and environmentally beneficial [6]. Compared to other traditional techniques, biosynthesis produces non-toxic by-products that increase NPs biocompatibility in various applications. Biological agents have emerged as good options for the

_____

generation of NPs due to their environmental friendliness, affordability, maintainability, and lack of chemical contamination [7-10]. Synthesis and engineering of nanoparticles by biological technique is dependent on several variants, the most significant variable is the shape of the metal nanoparticle to be produced [11]. Different factors, such as reaction time, reactant concentrations, pH, and temperature, can be used to control the morphological features of nanoparticles [12].

The most well-known uses of nanoparticles in the environmental field are removable arsenic from water wells [13]. Algae are an important source of a variety of commercial products, including natural colors and biofuels [14, 15]. Magnetic nanoparticles (NMs) have been shown to be beneficial in wastewater clean-up, owing to the unique features that make them superior to traditional treatment approaches. Magnetic, electrical, and optical properties, as well as catalytic activities, high reactivity, high mobility, and high adsorption capacities, are some of these qualities [16, 17]. The use of MNPs in the waste treatment sector has huge potential towards achieving greater efficiency of filtration materials, promoting reuse and recycling to a much greater extent [18]. The present research seeks to synthesize the more competent magnetic nanoparticle, comparing their adsorption capacity using *Chlorella* sp. and detecting the optimum condition for removing Cu^{+2} ion concentration in wastewater.

MATERIAL AND METHODS

Materials

BG11 (Blue green 11) medium, iron(II) sulfate heptahydrate ($FeSO_4.7H_2O$, Fluka, 86-90%), sodium nitrate ($NaNO_3$, Fluka, 99%), and sodium hydroxide (NaOH, Fluka, 99%), ammonia solution (NH_3, ALPHA, 99%), absolute ethanol (C_2H_5OH, GCC, 99.9%), tetraethyl orthosilicate (TEOS, $C_8H_{20}O_4Si$, Merck, ≥99%), acetic acid glacial (CH_3COOH, Scharlau, 99.8%), acetylacetone ($C_5H_8O_2$, Riedel-deHaën, 99.5%), tetra isopropyl orthotitanate (TIPO, $C_{12}H_{28}O_4Ti$, Merck, ≥98%) were used. All chemicals were analytical grade and were used without further purification. Hot plate and magnetic Stirrer (Shin Saeug co., Ltd, SHPM-10, TJ19-SHPM-11), oven (Memmert GmbH, U30, 801337), ultrasonic water bath (Powersonic 405, Hawshin technolog Co. Korea) were used. The FT-IR spectra were recorded on Shimadzu, FTIR spectroscopy Mod IR Affinity-1 CE, Japan using KBr disc at College of Education, Salahaddin University), scanning electron microscopy (SEM) and energy dispersive X-ray (EDX) were analyzed by Nova Nanosem 230 [FEI. USA], X-ray diffraction (XRD) type SRN-120M [SOONA, Korea] SRN-120 [SORONA, Korea]. The analytical techniques were used for the identification, and structural analysis, chemical and physical characterization of the samples were investigated in KURD central research facility.

Methods

Preparation of Chlorella biomass

Chlorella sp., received from the College of Health Sciences' microbiology lab, was purified on BG11 medium and incubated under continues light (1200Lx) at pH 7.2 and 23 °C. Two weeks later, following the growth of colonies on the agar media, the colonies were removed with pasture micropipettes and were gently blown into liquid medium then incubated at 23 °C, at pH 7.2. After 14 day filamentous cyanobacteria removed with pasture micropipette and examine under light microscope and examined under a light microscope to confirm its purity. The cultures in each flask were centrifuged to get biomass, the fresh biomass dried in an oven at 50 °C, and ground according to the manufacturer's instructions [19].

Preparation of ferrous(III) oxide Fe₃O₄ nanoparticle

The two solutions of (2.6 g (FeSO₄.7H₂O) and 2 g *Chlorella* sp. 25 mL distilled) was stirred and dissolved using a magnetic stirrer at 80 ºC, then 10 mL (2.5 M) NaOH solution was poured into the mixture with continuous stirring at 80 ºC for 30 min, the product was allowed to cool to room temperature before being washed and separated several times using an external magnetic field, and dried overnight at 50 ºC. The product of black color was weighed, yielding 76% of the nanoparticle [20]:

$$Fe^{+2} + 2Fe^{+3} + 8OH^- \rightarrow Fe(OH)_2 + 2Fe(OH)_3 \rightarrow Fe_3O_4 + 4 \ H_2O \qquad (1)$$
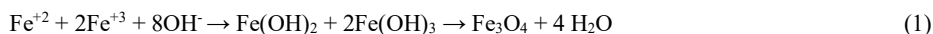
Preparation process of core-shell (Fe₃O₄/SiO₂) nanoparticles

The product ferrous(III) oxide Fe₃O₄ nanoparticles (45 mg) were ultrasonicated in 16 mL distilled water for 60 min, then 2 mL ammonium hydroxide (24 wt. percent) with 80 mL ethanol was added to the first solution, followed by adding 0.8 mL TEOS dropwise with stirring at room temperature for 24 hours, the nanoparticles washed and spread several times by external magnetic field with distilled water and the brown colored particle was dried and collected at 50 ºC [21].

Magnetic nanoparticles (MNps) characterization

The change of color in each core-shell Fe₃O₄/SiO₂ and core-shell Fe₃O₄ with *Chlorella* combinations was seen visually. Each sample was subjected to Fourier transforms infrared (FT-IR) analysis to validate nanoparticle production. Powdered samples were combined with potassium bromide and pressed into KBr pellets. The model infrared scan was generated at a resolution of cm⁻¹ in the mid-infrared range of 4000 to 400 wavenumbers. Furthermore, scanning electron microscopy (SEM), energy dispersive X-ray (EDX), and X-ray diffraction (XRD) were used to determine the size, shape, and composition of nanoparticles to offer information about the crystalline structure and grain size [22].

Copper removal using synthesized nanoparticles

Batch adsorption studies were conducted in a 250 mL conical flask containing 100 mL aqueous metal solution of the required concentration and known quantity of biosorbent. Initial pH was adjusted to the desired level with 1 N NaOH or 1 N HCl solution. Batch experiments were performed using different factors initial metal concentration (100-500 mg/L), pH (6.5-8.5), and temperature (20-40 ºC) according to [23]. Using a spectrophotometer at 680 nm with diphenylcarbazone reagent and H₂SO₄ to obtain the copper biosorption rate. The yield of removal and adsorption capacities for copper ion determined using the formula [23]:

Removal % of heavy metals = (C_o-C_e/C_o) × 100 (2)

The adsorption capacities were determined using equation 3:

$$q_e = [(C_\circ - C_e)V]/W \qquad (3)$$

where q_e is the amount of Cu(II) ion adsorbed per unit of nanoparticles (mg/g), C_o and C_e are the initial and equilibrium concentrations of Cu(II) ion in the solution (mg/L), V is the volume of Cu(II) ion solution (L) and W is the weight of the particle adsorbents (g).

Metal containing aqueous solution used as blank (control medium contained Cu(II) and distilled water without biosorbent to observe any reaction of the solution with metals).

RESULTS AND DISCUSSION

Chlorella harvesting

The pure culture of unicellular *Chlorella* sp. was received from a microbiology lab and sub-cultured on BG11 media examined under a microscope to verify the algal. The morphological characteristics of the current study were similar to the Iraqi strains of *Chlorella* identified by [24] which confirmed the strain and shows MNPs (Figure 1).
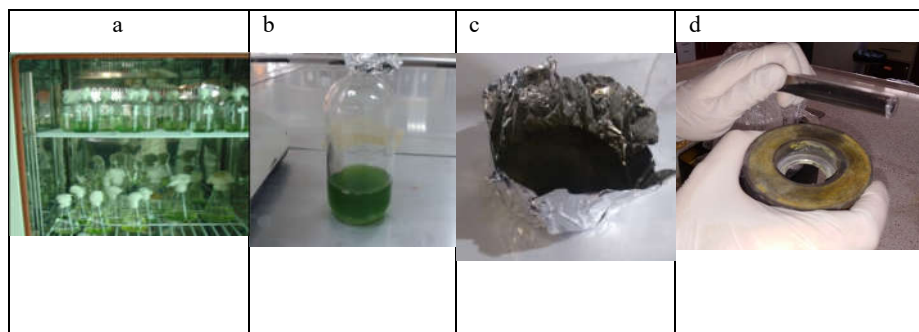

Figure 1. (a) *Chlorella* cultures, (b) *Chlorella* in BG-11 medium, (c) *Chlorella* biomass and (d) MNPs showing core-shell Fe_3O_4/SiO_2 with *Chlorella.*

Characterization of nanoparticles

The morphological observation showed in Figure 1d chemical and green synthesize of metallic nanoparticles ferrous(III) oxide Fe_3O_4 nanoparticle and Fe_3O_4 nanoparticle coated with SiO_2 appeared with *Chlorella* as black colure within temperature 80 °C. In algae, both photosynthesis and respiration are responsible for reducing metallic ions, which leads to the development of metallic nanoparticles within the [25]. The color change of mixture created at a specific temperature has been used as a visual indicator for the synthesis of silver and gold non-metals due to surface plasmon resonance, nano metals showed remarkable optical characteristics [26]. Mukherjee and his co-workers [27] conducted that the research of algae-mediated metallic nanoparticle production can be led to a new area of nanotechnology known as physco-nanotechnology.

The size of spherical magnetic Fe_3O_4 nanoparticle with *Chlorella* sp. is 59-72 nm has the specific surface area 25-15 m^2/g and the size of spherical magnetic Fe_3O_4 coated with SiO_2 and *Chlorella* spices is 88-110 nm with a specific surface area of approximately 15-6 m^2/g.

FTIR is a nondestructive, time-saving method for identifying different functional groups that is sensitive to molecular structural changes [28]. The FTIR information is based on chemical composition and physical state of the entire sample. Figure 2 shows the FTIR spectrum of magnetic nanoparticles. Strong absorption band appears around the region 600 cm^{-1} in FTIR spectra (a), and (b) are for stretching vibration of the Fe-O bending vibration, while the bands at 1082.07 cm^{-1} and 1066.64 cm^{-1} in the spectra (b) indicate non symmetrical shape without aggregation with the asymmetric stretching band for Si-O-Si. The small bands between 1400-1700 cm^{-1} are appeared in spectra (a) and (b), is for *Chlorella* functional groups like cellulose fatty acids $\nu(C=O)$ stretching of ester, protein amid bands $\nu(C=O)$ stretching, $\delta(N-H)$ bending and $\nu(C-N)$ stretching.
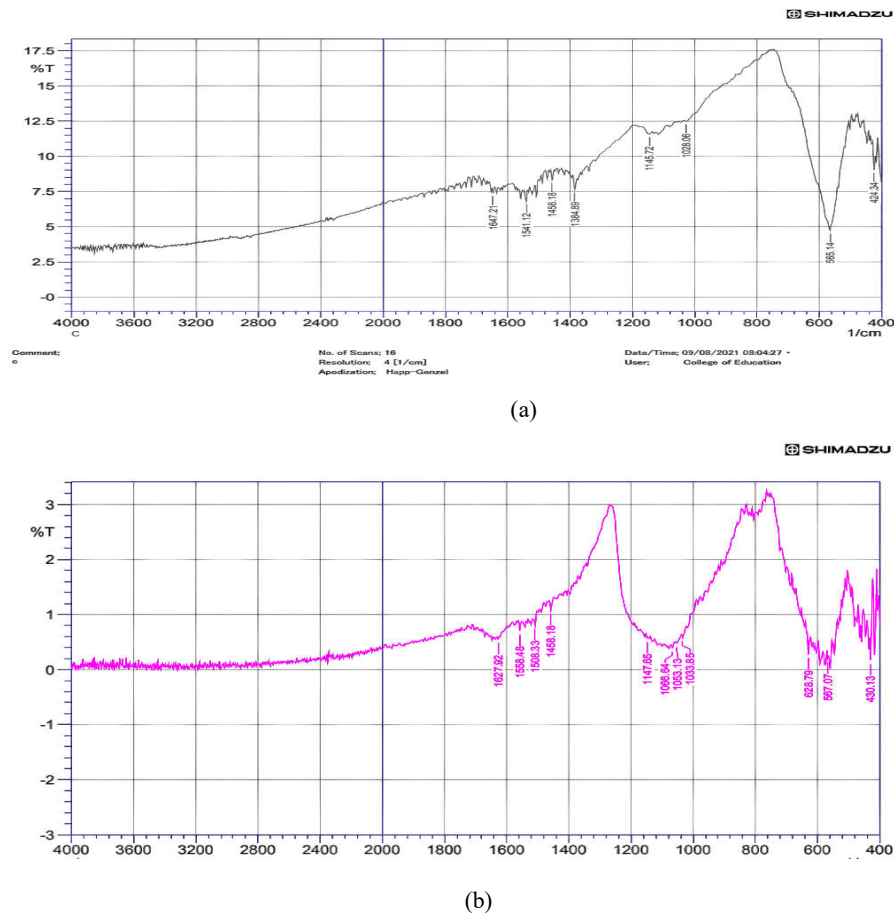
(a)

(b)

Figure 2. FTIR spectra of (a) core-shell Fe_3O_4 with *Chlorella* and (b) core-shell Fe_3O_4/SiO_2 with *Chlorella*.

Scanning electron microscopy (SEM) is an appropriate instrument for resolving individual MNPs and the structure of their linked nano trusses. Images of the produced nanoparticles have been obtained in various modulations. The SEM images shown with 100kx magnification all the nanoparticles have nonsymmetrical crystalline shape and the morphology of the magnetic nanoparticles with the surface of algae (*Chlorella*) were carried out on MIRA3 TESCAN (Figure 3). The average particle size of the magnetic nanoparticles was determined as follows Fe_3O_4 NPs prepared with *Chlorella* 59-72 nm, core-shell Fe_3O_4/SiO_2-*Chlorella* 88-110 nm the reason is that Fe_3O_4 is the core, its size is smaller 59-72 nm while Fe_3O_4/SiO_2 is the core Fe_3O_4 coated with SiO_2 core shell has larger size 88-110 nm. The morphology of magnetic nanoparticles was clearly observed by SEM in which the nanoparticles of the surface appeared as spherical to nonsymmetric crystalline shaped nanoparticles with agglomeration which may appear during processing with high temperature, Nandanwar and co-authors [29] indicated that the structural evolutions, crystallite size, and photodegradation performance of SiO_2 had a substantial link. SEM pictures

were used to investigate the structure of Fe_3O_4/SiO_2 and crystalline SiO_2 particles by Munasir and his colleagues [30]. The amorphous phase featured different particle sizes and morphologies than the crystalline phase, according to the findings. These findings were in line with what had been seen by Salem and co-authors [31].

MNPs attach to the surface of microalgal cells by nonspecific interactions such as electrostatic forces, hydrogen bonds, and hydrophobic and hydrophilic attractions. The magnetic property and tendency of MNPs to agglomerate produce the clustering of linked cells between the particles. [32-34].
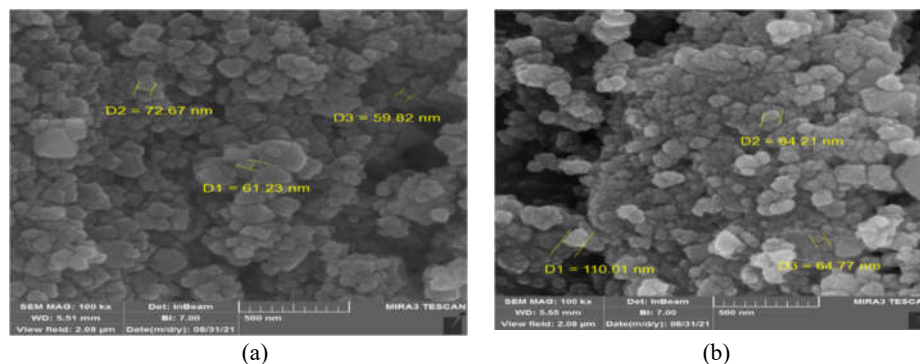

(a)   (b)

Figure 3. SEM manograph of (a) Fe_3O_4 with *Chlorella* and (b) core-shell Fe_3O_4/*Chlorella*/SiO_2.

The overviewing of energy dispersive X-ray used to illustrated the compositional information of each nanoparticle EDX spectra are shown in Figure 4 and the elemental analysis are presented in Table 1 where silicone element is found in spectra (b) core-shell Fe_3O_4/chlorella/SiO_2 with the percent 5.28% and 2.65%, respectively, indicating the shell of SiO_2, while a percent of other elements like carbon, nitrogen, sulfur, phosphor, potassium, magnesium and aluminum are presented in spectra (a and b) indicating the *Chlorella* functional groups. It contains proteins (up to 60% of dry weight), polysaccharides (10–15%), lipids (12–15%), unsaturated fatty acids, and carotenoids (predominantly lutein), as well as some immunostimulators, vitamins, and minerals.

Table 1. The quantitative EDAX analysis for each biosynthesized material.

Materials	Element (atom %)										
	Fe	O	Si	C	N	Na	Al	P	S	Mg	Total
Fe_3O_4	53.06	32.71		8.81	3.69	1.2	0.23	0.04	0.25		100
Core-shell Fe_3O_4-SiO_2	53.28	30.8	2.65	7.70	5.29		0.22			0.06	100

The XRD images are indexed in Figure 5 are characterized successfully and agree with the standard XRD spectrum. The peaks at $2\theta = 31°$, 35.6°, 43.5°, 53.5°, 57.3°, and 62.9° were allocated to (220), (311), (400), (422), (511) and (440) reflections, respectively. These peaks were also observed in the spectrum of core-shell Fe_3O_4/SiO_2 NPs, and no peaks conformable to impurities are obtained.
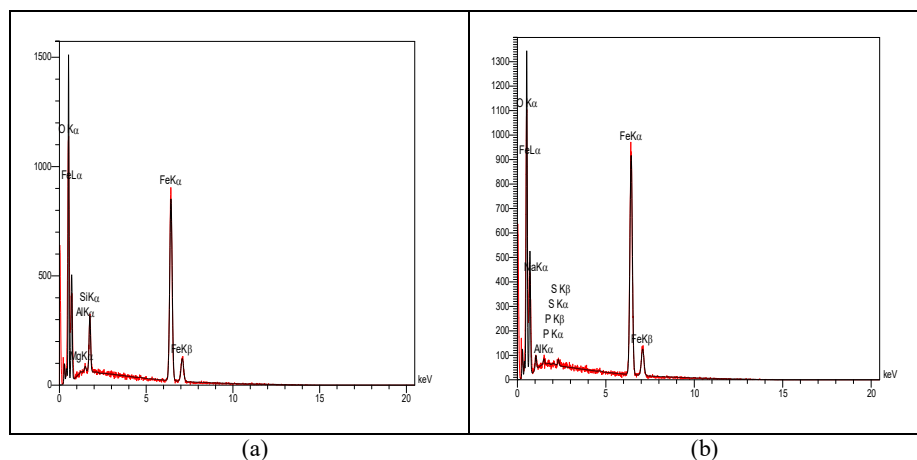
(a)   (b)

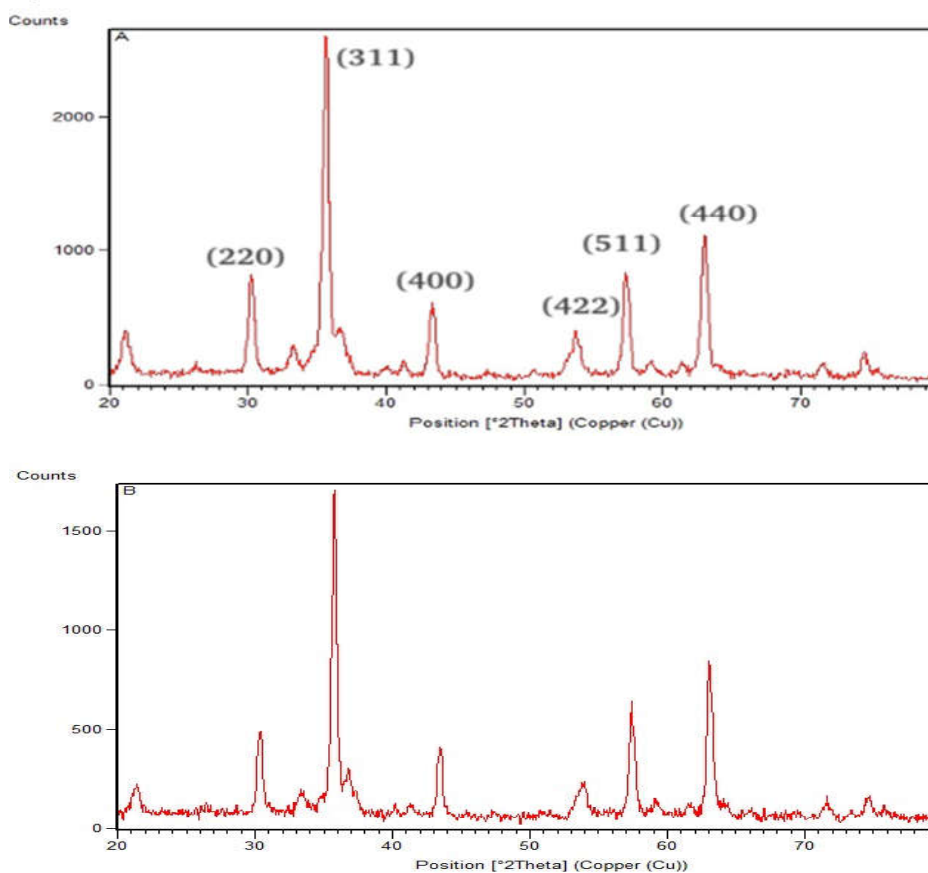Figure 4. EDX of a- Fe₃O₄ with *Chlorella*, b- core-shell Fe₃O₄/*Chlorella*/SiO₂.

Figure 5. XRD of (A) Fe₃O₄ and (B) core-shell Fe₃O₄/SiO₂.

Effect of Cu^{+2} ion concentrations on biosorption

The effect of the initial metal ion concentration (Cu^{+2}) in the range (100 mg/L) for both prepared nanoparticles showed in Figure 6. The maximum removal is displayed for 5 hours, and the fast removal has been showed during 2 min (83%). The maximum adsorption of Cu^{+2} was recorded with MNPs if compared with cell surface of Chlorella (35.4%). By increasing metal concentration, the biosorption process is reduced the competitive dispersion of metal ions has risen at the sites available on the adsorbent surface at high concentrations; these pores are closed, and metal ions are prevented from going deep into the absorbent pores, implying that adsorption occurs exclusively on the surface [35].
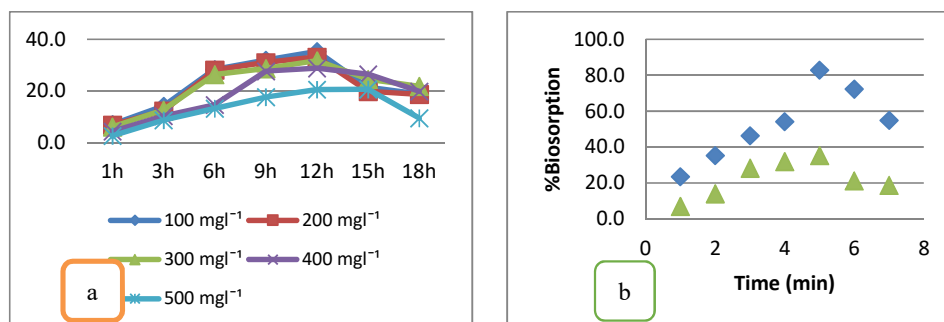

Figure 6. Effect of copper concentration on biosorption process by (a) *Chlorella sp.* and (b) Fe$_3$O$_4$ prepared with *Chlorella* sp., core-shell Fe$_3$O$_4$/SiO$_2$ with *Chlorella* sp.

Effect of pH on biosorption of Cu^{+2}

One of the most critical factors determining the initial adsorption rate and strength is pH. This effect is due to the nature of the chemical reaction between each heavy metal and the cell surface. The hydrogen ion also acts as a link between the heavy metal compounds and the microalgal cell wall. The effect of the initial pH on the adsorption capacity and removal of Cu^{+2} by using magnetic nanoparticles prepared with *Chlorella* is given in Figure 7 and Table 2. Maximum removal of Cu^{+2} showed during 6 min at pH 8 (85%) by *Chlorella* coated with core-shell Fe$_3$O$_4$/SiO$_2$. It was determined that the adsorption of Cu^{+2} increased as the pH value increased because at lower pH, the solution included more hydrogen ions (H+), and the high concentration was competitive with both metal ions, resulting in poor adsorption [36, 37]. Wanta and his friends [38] confirmed that the biosorption of Cu^{+2} was increased with increasing the pH value.

Effect of temperature on Copper ion adsorption

The effect of temperature on removal of Cu^{+2} and adsorption capacity by both prepared nanoparticles shown in Figure 8 and Table 2. The maximum removal was observed within 4 min at 25 °C (86.9%) by *Chlorella* coated with core-shell Fe$_3$O$_4$/SiO$_2$, and rapid removal showed after 1 min at a temperature (19%). The increase of adsorption with increased temperature indicated that the adsorption of heavy metal ions by adsorbent may involve not only physical [39] reported that the optimum temperature for removal of Cu^{+2} was at 25 °C. Giraldo *et al.* used co-precipitation methods for the treatment of Pb(II), Cu(II) and the results demonstrated that nano sized magnetite had the best adsorption effect.
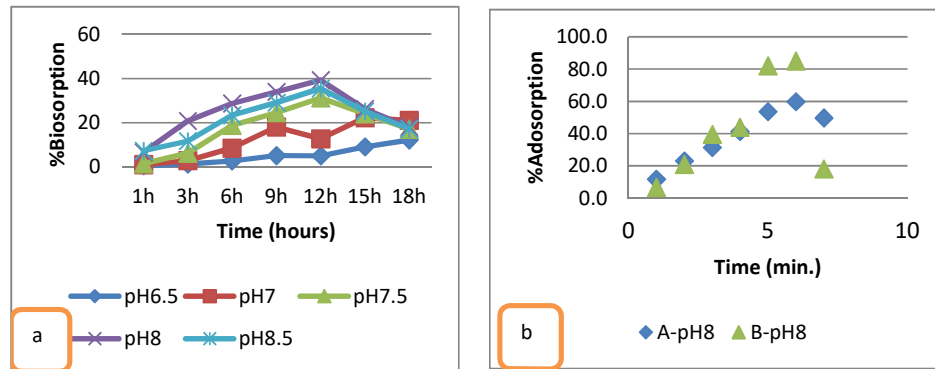
Figure 7. Effect of pH on biosorption process by (a) Chlorella sp. and (b) Fe$_3$O$_4$/*Chlorella* sp. and Core-shell Fe$_3$O$_4$/SiO$_2$ with *Chlorella* sp.
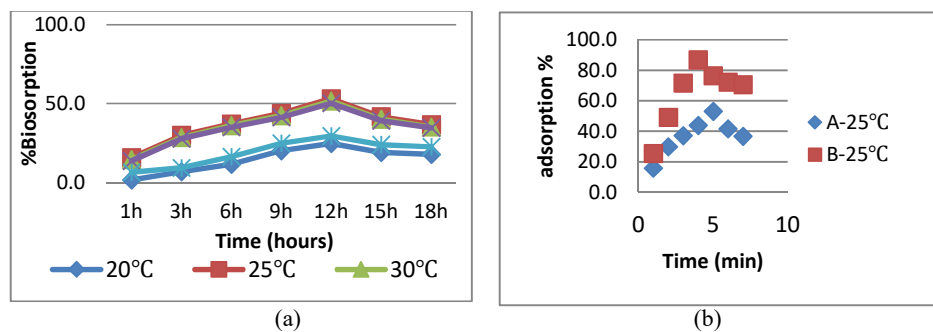

Figure 8. Effect of temperature on biosorption process by (a) *Chlorella* sp., and (b) Fe$_3$O$_4$/*Chlorella* sp and core-shell Fe$_3$O$_4$/SiO$_2$ with *Chlorella sp.*

The adsorption rate was rapid during the initial time periods. Equilibrium times of 1 and 6 min were required for the adsorption of copper ions which is very rapid method, and the maximum removal obtained with core-shell Fe$_3$O$_4$/SiO$_2$ with *Chlorella* sp. (Table 2|.

Table 2. Biosorption capacity of copper(II) ion by synthetic and biosynthetic nanoparticles.

Materials	C$_o$ (mg/L)	Time (h)	C$_e$ (mg/L)	q$_e$ (mg/g)	% Biosorption
Core-shell Fe$_3$O$_4$/SiO$_2$ core prepared with *Chlorella* sp.	112	9	97.3	0.28	86.9
Fe$_3$O$_4$ prepared with *Chlorella* sp.	132	9	106	0.25	80.3

CONCLUSION

As indicated by a large number of published researches over the preceding years, nanotechnology has achieved substantial progress in several areas, including water purification and heavy metal

removal. As a result, a framework for heavy metal removal from water using the adsorption technique is needed, one that encompasses not just the important findings of the preceding decade, but also all facets of the process. After treatment with a magnetic field, the magnetite readily separated from the aqueous solution. The easiest way of production of iron oxides is co-precipitation, as can be seen from the numerous approaches. The optimal pH and temperature for maximal copper(II) adsorption were pH 8 and 25 ºC, respectively. After desorption, the capacity to reuse nanoparticles is an essential application feature. As a result, each adsorbent must be created with the purpose of employing the adsorption process to remove a specific pollutant.

ACKNOWLEDGMENT

REFERENCES

1. Majidi, S.; Sehrig, F.Z.; Farkhani, S.M.; Goloujeh, M.S.; Akbarzadeh, A. Current methods for synthesis of magnetic nanoparticles. *Artif. Cells Nanomed. Biotechnol.* **2016**, 44, 722-734.
2. Davaran, S.; Akbarzadeh, A.; Nejati-Koshki, K.; Alimohammadi, S.; Ghamari, M.F.; Soghrati, M.; Rezaei, A.; Khandaghi, A.A. In vitro studies of Nipaam-Maa-Vp copolymer-coated magnetic nanoparticles for controlled anticancer drug release. *J. Encapsulation adsorpt. Sci* **2013**, 3, 108-115.
3. Mahdavi, M.; Namvar, F.; Ahmad, Mb.; Mohamad, R. Green biosynthesis and characterization of magnetic iron oxide (Fe$_3$O$_4$) nano particles using seaweed (*Sargassum muticum*) aqueous extract. *Molecules* **2013**, 18, 5954-5964.
4. Tesfaw, B.; Chekol, F.; Mehretie, S.; Admassie, S. Adsorption of Pb(II) ions from aqueous solution using lignin from *Hagenia abyssinica*. *Bull. Chem. Soc. Ethiop.* **2016**, 30, 473-484.
5. Brown, An.; Smith, K; Samuels, Ta; Lu, J; Obare, So; Scott, Me. Nanoparticles functionalized with ampicillin destroy multiple-antibiotic-resistant isolates of *Pseudomonas aeruginos*a and *Enterobacter aerogenes* and methicillin-resistant *Staphylococcus aureus*. *Appl. Environ. Microbiol.* **2012**, 78, 2768-2774.
6. Zhang, D.; Ma, X.; Gu, Y.; Huang, H.; Zhang, G. Green Synthesis of Metallic Nanoparticles and Their Potential Applications to Treat Cancer. *Front. Chem.* **2020**, 8, Article 799.
7. Ahmed, S.; Annu, H.; Ikram, S.; Yudha, S. Biosynthesis of gold nanoparticles: A green approach. *J. Photochem. Photobiol.* **2016**, 161, 141-153.
8. Al-Bahrani, L.; Hassan, A.; Sabaratnam, V. Green synthesis of silver nanoparticles using tree oyster mushroom *Pleurotus ostreatus* and its inhibitory activity against pathogenic bacteria. *Mater. Lett.* **2017**, 186, 21-25.
9. Costa Silva, L.; Oliveira, P.; Keijok, W.; Da Silva, R.; Aguiar, R.; Guimarães, M.C.; Ferraz, C.M.; Araújo, J.V.; Tobias, F.L.; Braga, F.R. Extracellular biosynthesis of silver nanoparticles using the cell-free filtrate of nematophagous fungus *Duddingtonia flagrans*. *Int. J. Nanomedicine* **2017**, 12, 6373-6381.
10. Kim, D.; Saratale, Rg.; Shinde, S.; Syed. A.; Ameen, F.; Ghodake, G. Green synthesis of silver nanoparticles using *Laminaria japonica* extract: Characterization and seedling growth assessment. *J. Clean Prod.* **2018**, 172, 2910–2818.
11. Gahlawat, G.; Choudhury, R. A review on the biosynthesis of metal and metal salt nanoparticles by microbes. *RSC Adv.* **2019**, 9, 12944-12967.
12. Raychaudhuri, R.; Pandey, A.; Hegde, A.; Abdul Fayaz, S.; Chellappan, K.; Dua, K.; Mutalik S. Factors affecting the morphology of some organic and inorganic nanostructures for drug

delivery: Characterization, modifications, and toxicological perspectives. *Expert Opin. Drug Deliv.* **2020**, 17, 1737-1765.

13. Bucurica, I.; Popescu, I.; Radulescu, C.; Valerica, G.; Dulama, I.; Teodorescu, S.; Gurgu V.; Let, D. Investigation of metallic nanoparticles adsorbed on the QCM sensor by SEM and AFM techniques. *Bull. Mater. Sci.* **2018**, 41, 71.

14. Borowitzka, Ma; High-value products from microalgae—their development and commercialisation. *J. Appl. Phycol.* **2013**, 25, 743-756.

15. Sharma, A.; Sharma, S.; Sharma, K.; Chetri Spk, A.; Singh, P.; Kumar, R.; Rathi, B. Agrawal, V. Algae as crucial organisms in advancing nanotechnology: A systematic review. *J Appl Phycol.* **2016**, 28, 1759-1774.

16. Peigneux, A.; Puentes-Pardo, D.; Rodríguez-Navarro, B.; Hinckeet, M.; Jimenez-Lopez, P. Development and characterization of magnetic eggshell membranes for lead removal from wastewater. *Ecotoxicol. Environ. Saf.* **2020**, 192, 110307.

17. Shukla, S.; Khan, R.; Hussain, M. *Nanoremediation. The Handbook of Environmental Remediation*, Royal Society of Chemistry: London; **2020**, pp. 443-467. DOI: 10.1039/9781788016261-00443.

18. Reddy, L.; Arias L.; Nicolas, J.; Couvreur, P.; Magnetic nanoparticles: Design and characterization, toxicity and biocompatibility, pharmaceutical and biomedical applications. *Chem. Rev.* **2012**, 112, 5818–5878.

19. Abdulkareem, M.; Anwer, S. Biosorption of cadmium and lead using microalgae *Spirulina* sp. isolated from Koya City (IRAQ). *Appl. Ecol. Environ. Res.* **2020**, 18, 2657-2668.

20. Majeed, M.; Guo, J.; Yan, W., Tan, B. Preparation of magnetic iron oxide nanoparticles (MIONs) with improved saturation magnetization using multifunctional polymer ligand. *Polymers* **2016**, 8, 392.

21. Han, J.; Seok, G. A preparation of dual-layered core–shell Fe$_3$O$_4$-SiO$_2$ nanoparticles and their properties of plasmid DNA purification. *Nanomaterials* 2021, 11, 3422.

22. Slater, T.; Janssen, A.; Camargo, P.; Burke, M.; Zaluzec, N.; Haig, S. STEM-EDX tomography of bimetallic nanoparticles: A methodological investigation. *Ultramicroscopy* **2016**, 167, 63-71.

23. Abdulkareem, M. Induced wastewater treatment and biodiesel production using microalgae isolated from Koya distinct. *PhD Thesis*, Koya University, Koya, Iraq, **2020**.

24. Anwer, S.S.; Sdiq K.S.; Muhammad, K.R. Aladdin M.A. Phenolic compound and fatty acid properties of some microalgae species isolated from Erbil City. *Braz. J. Biol.* **2022**, 82, e256927.

25. Jena, J.; Pradhan, N.; Nayak, R.R.; Dash, B.P.; Sukla, L.B.; Panda, K.; Mishra, K. Microalga *Scenedesmus* sp.: A potential low-cost green machine for silver nanoparticle synthesis. *J. Microbiol. Biotechnol.* **2014**, 24, 522-533.

26. Borah, D.; Das, N.; Das, N.; Bhattacharjee, A.; Sarmah, P.; Ghosh, K.; Chandel, M.; Rout, J.; Pandey, P.; Ghosh, N. Alga-mediated facile green synthesis of silver nanoparticles: Photophysical, catalytic and antibacterial activity. *Appl. Organomet. Chem.* **2020**, 34, e5597.

27. Mukherjee, A.; Sarkar, D.; Sasmal, S. A review of green synthesis of metal nanoparticles using algae. *Front. Microbiol.* **2021**, 12, 693899.

28. Fatima, H.; Lee, D.; Yun, H.; Kim, K. Shape-controlled synthesis of magnetic Fe$_3$O$_4$ nanoparticles with different iron precursors and capping agents. *RSC Adv.* **2018**, 8, 22917-22923.

29. Nandanwar, R.; Singh, P.; Fozia, Z. Synthesis and characterization of SiO$_2$ nanoparticles by sol-gel process and its degradation of methylene blue. *Am. Chem. Sci. J.* **2015**, 5, 1-10.

30. Munasir; Dewanto, A.S.; Kusumawati, D.H.; Putri, N.P.; Yulianingsih, A.; Saadah, I.K.F.; Taufiq, A.; Hidayat, N.; Sunaryono, S.; Supardi, Z.A. Structure Analysis of Fe3O4@SiO2 Core Shells Prepared from Amorphous and Crystalline SiO2 Particles. IOP Conf. Ser.: *Mater. Sci. Eng.* **2018**, 367, 012010. https://doi.org/10.1088/1757-899X/367/1/012010.

31. Salem, D.M.; Ismail, M.M.; Aly-Eldeen, M.A. Biogenic synthesis and antimicrobial potency of iron oxide (Fe_3O_4) nanoparticles using algae harvested from the Mediterranean Sea, Egypt. *Egypt. J. Aquat. Res.* **2019**. 45, 197-204.

32. Chatterjee, S.; Bandyopadhyay, A.; Sarkar, K. Effect of iron oxide and gold nanoparticles on bacterial growth leading towards biological application. *J. Nanobiotechnol.* **2011**, (9), 34.

33. Ebrahiminezhad, A.; Varma, V.; Yang, S.; Ghasemi, Y.; Berenjian, A. Synthesis and application of amine functionalized iron oxide nanoparticles on Menaquinone-7 fermentation: A Step towards Process Intensification. *Nanomaterials* **2016**, 6, 1.

34. Habib N.R.; Taddesse, A.M.; Temesgen, A. Synthesis, characterization and photocatalytic activity of $Mn_2O_3/Al_2O_3/Fe_2O_3$ nanocomposite for degradation of malachite green. *Bull. Chem. Soc. Ethiop.* **2018**, 32, 101-109.

35. Zhou, G.; Peng, F.; Zhang, L.; Ying, G. Biosorption of zinc and copper from aqueous solutions by two freshwater green microalgae *Chlorella pyrenoidosa* and *Scenedesmus obliquus*. *Environ. Sci. Pollut. Res. Int.* **2011**, 19, 2918-2929.

36. Manimozhi, V.; Partha, N.; Sivakumar, E.; Jeeva, N.; Jaisankar, V. Preparation and characterization of ferrite nanoparticles for the treatment of industrial waste water. *Digest J. Nanomater. Biostruct.* **2016**, 11, 1017-1027.

37. Wambu, E.; Attahiru, S.; Shiundu M.; Wabomba J. Removal of heavy-metals from wastewater using a hydrous alumino-silicate mineral from Kenya. *Bull. Chem. Soc. Ethiop.* **2018**, 32, 39-51.

38. Wanta, K.; Hidayat, C.; Miryanti, A.; Kristijarti, A. Biosorption of copper(II) ions using living *Chlorella* sp. from aqueous solution. IOP Conf. Ser.: Mater. Sci. Eng. 2020, IOP Publishing, 012026. DOI: 10.1016/s0045-6535(01)00324-1.

39. Wan Maznah, W.O.; Al-Fawwaz, A.T.; Surif, M. Biosorption of copper and zinc by immobilised and free algal biomass, and the effects of metal biosorption on the growth and cellular structure of *Chlorella* sp. and *Chlamydomonas* sp. isolated from rivers in Penang, Malaysia. *Res. J. Environ. Sci.* **2012**, 24, 1386-1393.